Article

Pyroelectricity and related properties in the fresnoite pseudobinary system $Ba_2TiGe_2O_8$-$Ba_2TiSi_2O_8$

SCHMID, Hans, *et al*.

Abstract

Complete solid solubility is found in the pseudobinary system Ba2TiGe2O8-Ba2TiSi2O8 by making studies on ceramics and single crystals (Czochralski technique). The spontaneous birefringence perpendicular to the polar axis of the orthorhombic low temperature phase was measured vs. temperature and Si contents: the temperature of the phase transition of species 4mmFmm2 is of 2nd order and decreases from 1103 K at 0 at.% Si to about 400 K at 40 at.% Si. The pyroelectric coefficient in the orthorhombic mm2 and the tetragonal 4mm phases is of the order of 10-6 C m-2 K-1 in the entire system and all compositions studied have a positive temperature coefficient except Ba2TiGe2O8, in which the pyroelectric coefficient changes sign at .apprx. 308 K. The proposed space group of the orthorhombic phase is C2v11-Cmm2.

Reference

SCHMID, Hans, *et al*. Pyroelectricity and related properties in the fresnoite pseudobinary system $Ba_2TiGe_2O_8$-$Ba_2TiSi_2O_8$. *Journal of materials science*, 1978, vol. 13, no. 10, p. 2257-2265

DOI : 10.1007/BF00541682

JOURNAL OF MATERIALS SCIENCE 13 (1978) 2257–2265

Pyroelectricity and related properties in the fresnoite pseudobinary system $Ba_2TiGe_2O_8$-$Ba_2TiSi_2O_8$

H. SCHMID,* P. GENEQUAND, H. TIPPMANN, G. POUILLY, H. GUÉDU
Battelle Geneva Research Laboratory, CH-1227 Carouge-Geneva, Switzerland

Complete solid solubility is found in the pseudobinary system $Ba_2TiGe_2O_8$–$Ba_2TiSi_2O_8$ by studies on ceramics and single crystals (Czochralski technique). The spontaneous birefringence perpendicular to the polar axis of the orthorhombic low temperature phase has been measured versus temperature and silicon contents: the temperature of the phase transition of species 4mmFmm2 is of second order and decreases from 1103 K at 0 at % Si to about 400 K at 40 at % Si. The pyroelectric coefficient in the orthorhombic mm2 and the tetragonal 4 mm phase is of the order of 10^{-6} C m^{-2} K^{-1} in the entire system and has a positive temperature coefficient for all compositions studied except for $Ba_2TiGe_2O_8$, in which the pyroelectric coefficient changes sign at about 308 K. The spacegroup of the orthorhombic phase is proposed to be C_{2v}^{11}–Cmm2.

1. Introduction

The germanium fresnoite $Ba_2TiGe_2O_8$ was reported [1] to exhibit a phase transition (DTA bend at 850° C and minimum of piezoelectric resonance frequency at 810° C) from a polar tetragonal high temperature phase to a ferroelastic polar orthorhombic phase, characterized by the Aizu species [2] 4mmFmm2. There exist three main types of phase transition with polar prototype symmetry [2, 3]. Their respective low-temperature phases are characterized by the following property combinations: (i) fully ferroelectric/fully ferroelastic; (ii) non-ferroelectric/fully ferroelastic, and (iii) non-ferroelectric/non-ferroelastic.

For the case of these polar–polar transitions, "non-ferroelectric" is understood in the sense that the spontaneous polarization of the low temperature phase domains is neither divertible nor reversible, i.e., all domains necessarily have the same orientation of the dipole moment owing to a symmetry conditioned, "inbuilt bias". Therefore cycling through the temperature of the phase transition would never lead to depoling. In consequence, such materials would be highly interesting as robust pyroelectric single element detectors or imaging target materials provided the pyroelectric figure of merit requirements were met.

From the symmetry point of view, the non-ferroelastic species of type (iii) are most desirable because their domains would necessarily be stress-free and pyroelectrically indistinguishable. Apparently no example of a pure compound, belonging to this type, is known.

Species of type (ii) are somewhat less favourable because the ferroelastic character of the domains can in principle lead to stressed domain patterns which may induce slight differences of pyroelectric coefficient in the vicinity of the domain walls, and thus lead to their visualization if the crystal is used as an imaging target. Germanium-fresnoite $Ba_2TiGe_2O_8$ seems to be the only known example of type (ii), whereas lithium ammonium sulphate, initially thought to possess species mm2F2 [3] (hence of type (ii)), has recently been found to possess in reality a different type of transition [4].

*Present address: Department of Inorganic, Analytical and Applied Chemistry, University of Geneva, quai Ernest-Ansermet, CH-1211 Geneva 4, Switzerland.

The work presented in this paper was intended to study the nature of the phase transition of germanium fresnoite and to examine whether by formation of mixed crystals with silicon fresnoite the transition temperature, and thus a possible anomaly of pyroelectric coefficient, might be lowered so as to lead to a composition pyroelectrically useful at room temperature.

2. Experimental

2.1. Ceramics

The synthesis of ceramic material was necessary for several purposes: differential thermoanalysis (DTA), thermogravimetry (TG), X-ray analysis, dielectric measurements and starting material for single crystal growth.

2.1.1. Preparation of ceramic material

The starting materials were TiO_2 Fluka/Buchs "purum" ($\geqslant 99\%\ TiO_2$), $BaCO_3$ Merck, Darmstadt "pro analysi" ($BaCO_3 \geqslant 99\%$), GeO_2 Fluka "puriss" (99.999%) and SiO_2 (quartz powder). The conditions and steps of the synthesis were as follows: *mixing* of the powders in a ball mill (Al_2O_3 balls, suspension in acetone, 2 h) → *air drying* (~ 120° C) → *calcination* (Al_2O_3 vessel, air, 1000° C, 24 h) → *crushing* (in agate mortar) → *ball, milling* (Al_2O_3 balls, in acetone, 2 h) → *air drying* → *isostatic pressing* (10 tons cm^{-2}, glycerine, samples in tight plastic foil) → *sintering* (ordinary atmosphere, platinum support).

The sintering conditions were as given in Table I. The compositions with 80 and 100 at.% Si showed traces of β-$BaSiO_3$ after sintering at 1175° C, but which disappeared after crushing and resintering at 1365° C (see Section 2.1.2.1.).

TABLE I Sintering conditions

Composition (at.% Si)	Temperature/time (° C/h)
0, 20, 30, 35	1175/24
40	1175/24 → 1200/12
60	1175/24 → 1275/12 → 1300 (24)
80	1175/24 → crushing, milling → 1320/24
100	1175/24 → crushing, milling → 1365/24

2.1.2. Characterization of ceramic material

2.1.2.1. X-ray powder analysis. All prepared ceramic compositions were analysed with CuKα radiation in the d-value range of 1.32 to 4.40 Å. The reflections of all compositions could be explained by the tetragonal indexation given for $Ba_2TiSi_2O_8$ [5, 6]. In the indexation given for $Ba_2TiGe_2O_8$ [7], we found the rather strong reflection $(3\,2\,0)_{tetr.}$ with $d = 2.40$ to be omitted, and the reflection $(2\,1\,2)/(3\,2\,1)$ to be erroneous with $d = 2.26$ instead of 2.21.

The compositions between 0 and 60 at.% Si were characterized by two very weak reflections at $d = 3.40$ and $d = 3.45$ which could not be assigned to the tetragonal symmetry. They probably belong to the orthorhombic structure. The tetragonal reflections do not show any splitting for d-values equal to or higher than 1.32. The ferroelastic shear of the orthorhombic phase must therefore be very small.

2.1.2.2. Differential thermal analysis (DTA) and thermogravimetry (TG). The sintered samples were analysed by DTA and TG using a "Mettler thermoanlyser 1" and heating rates of both 8 and 4° C min^{-1}. The temperatures of the melting point (taken at the peak of the DTA anomaly) were reproducible on heating only and lay on a nearly straight line between the Ge and the Si fresnoite (Figs. 1 and 12). Solidification was not found to

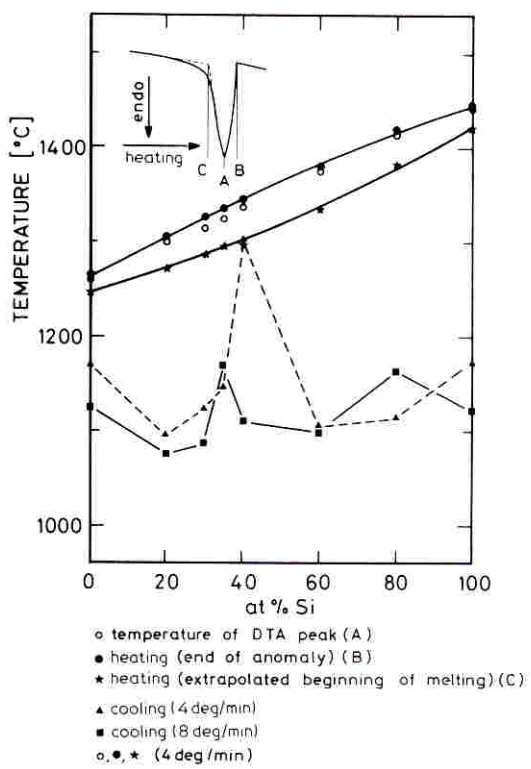

Figure 1 Temperatures of fusion (at 4° C min^{-1}) and solidification at 4 and 8° C min^{-1}. The drawn links between the solidification temperatures are of no physical significance.

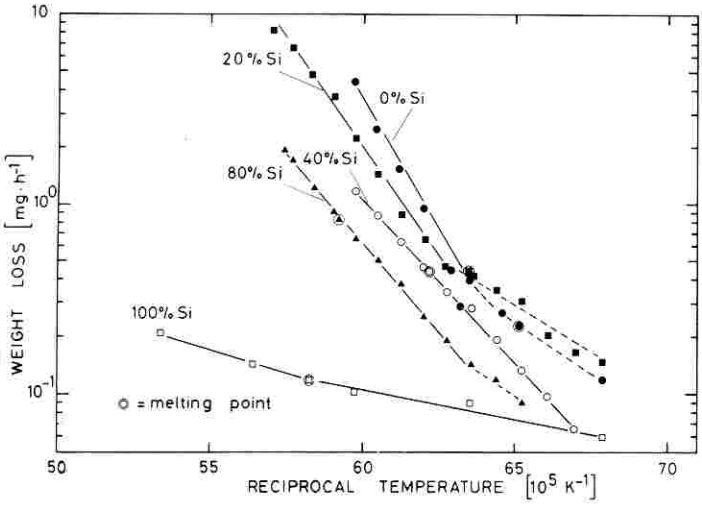

Figure 2 Weight (log scale) during DTA runs of various fresnoite compositions versus reciprocal temperature.

be reproducible, was cooling rate dependent, and affected by strong supercooling of ~100 to 300° C (Fig. 1). The solidus equilibrium curve could therefore not be determined accurately. Only an approximate curve (Fig. 1) has been obtained by extrapolating the DTA curve on heating in the way shown on the inset of Fig. 1.

The melting points observed for Ge and Si fresnoite, 1260° C and 1439° C, respectively, are consistent with the respective literature data of 1260° C [8] and 1445 ± 5° C [9, 10]. Kimura *et al.* [1] found a small bend of the DTA curve (heating rate 19° C min^{-1}) of $Ba_2TiGe_2O_8$ at 850° C, indicating the transition 4mmFmm2. Unfortunately our DTA curves, even if run at the greatest possible speed of 15° C min^{-1}, did not show up the phase transition. It therefore became necessary to produce small single crystals and to determine the transition as a function of the Si/Ge ratio by means of a polarizing microscope (see Section 2.2.2.3).

The registered weight loss during the DTA runs is plotted in a log (weight loss)–reciprocal temperature diagram in Fig. 2, without correction for buoyancy and reversibility. The curve for the pure Si-fresnoite was found to be reversible on cooling (owing to buoyancy or degassing). The curve of the compositions containing GeO_2 have a much steeper slope and indicate a real loss of GeO_2. Similar loss curves of GeO_2 are found for GeO_2 containing garnets [11].

2.1.1.3. Dielectric constant of ceramic. In an attempt to localize the temperature of the phase transition, the dielectric constant was measured on some sintered samples. At 40 at.% Si (Fig. 3) a

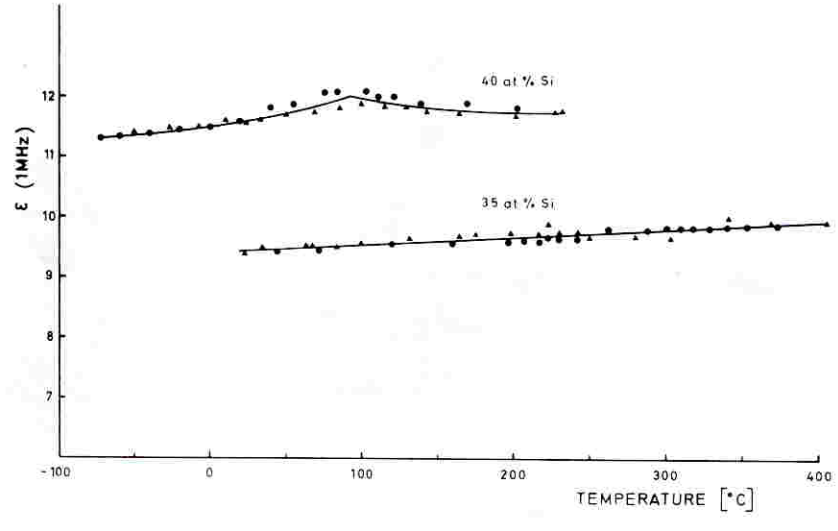

Figure 3 Dielectric constant (1 MHz) of ceramic fresnoites of 35 and 40 at.% silicon versus temperature.

TABLE II Some typical pulling conditions of $Ba_2TiGe_{2-2x}Si_{2x}O_8$ crystals ($0 \leq x \leq 0.6$)

Ge/Si ratio (at.% Si)	Temperature (°C)		Axial thermal gradient* (°C cm^{-1})	Speed of rotation (r.p.m.)	Pulling speed (mm h^{-1})	Diameter/ length of crystal (ϕ, mm/L, mm)	Remarks
	Crucible wall	DTA peak					
0	1274	1260	50	105	1	7/14	Smooth surface, 3 grains
20	1304	1298	20	25	2	7.5/24	Cellular growth, several grains $(1\,1\,0)_{tetr.}$ facets
30	1321	1324	20	25	2 5	5/30	Cellular growth, 2 grains $(1\,1\,0)_{tetr.}$ facets
35	1329	1324	30	105	1 2	4/23	Smooth surface, 1 grain, well transparent
40	1348	1337	20	25	2 3	/12	Smooth surface, 2 grains, cellular growth
60	1383	1376	20	12	12 17	8/53	Several grains, $(1\,1\,0)_{tetr.}$ facets

*At surface of melt.

small bend was found at about 90° C, suggestive of the transition, whereas at 35 at.% Si (Fig. 3) no anomaly was detected up to 400° C. Compositions with less Si content could not be measured around T_t because of limitation of the equiment.

2.2. Single crystals

2.2.1. Preparation

Single crystals of compositions with 0, 20, 30, 35, 40 and 60 at.% Si (nominal) have been grown by the Czochralski technique, in air, using a SiC tubular heater element (Crusilite/Morganite Comp.), an Al_2O_3 protective tube, a cylindrical platinum crucible ($\phi = 28$ mm, height = 40 mm) and temperature stabilization of better than one degree. Temperature measurement was made with a Pt–Pt/Rh thermocouple welded to the crucible wall. Pulling conditions and dimensions obtained are given in Table II.

2.2.2. Characterization of single crystals

2.2.2.1. External and internal aspect. Whereas it was relatively easy to pull crystals with 100 at.% Ge (Fig. 4), the mixed crystals usually showed a cellular structure (Fig. 5) with inhomogeneous Si/Ge ratio as monitored by differences in spontaneous bi-refringence (Fig. 6). This effect is due to constitutional supercooling (see e.g. [12]) and can in principle be eliminated by a high axial thermal gradient and a very low pulling rate (see e.g. [13]). However, the resistance heating system

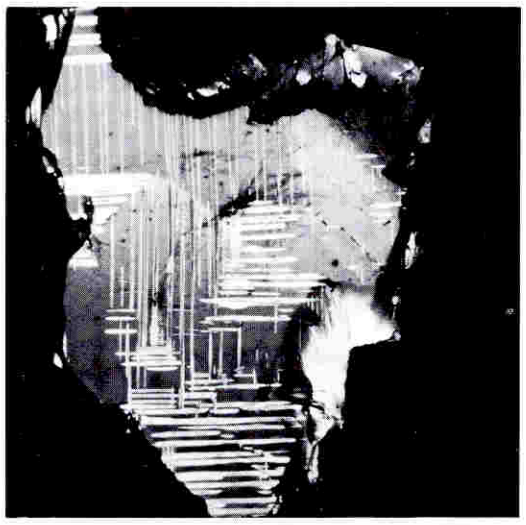

Figure 4 Platelet of $Ba_2TiGe_2O_8$, (0 0 1) cut, viewed in polarized light (45° position). It consists of two slightly mutually misoriented blocks. Some spikes, running vertically through the small angle boundary, show bends.

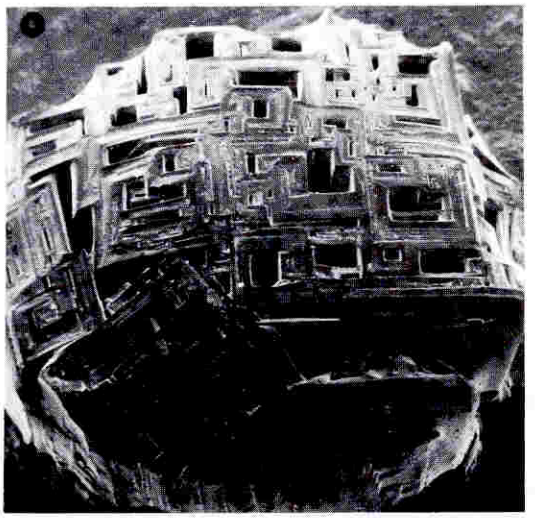

Figure 5 Cellular structure of growth interface of a fresnoite with 30 at. % Si (Stereoscan, 18 ×).

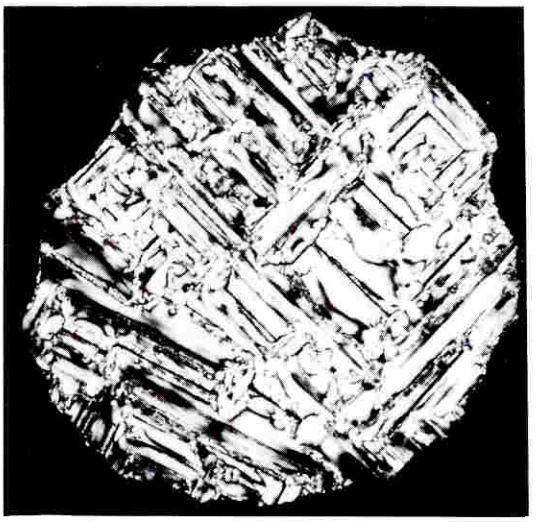

Figure 6 Fresnoite platelet, (0 0 1) cut, with 30 at. % Si (nominal) viewed in polarized light (45° position), showing cellular structure. The lower left-hand part has a different orientation.

used did not allow such high gradients (90 to 150° C min^{-1}) as have been used for Si- and Ge-fresnoite Czochralski growth by means of induction heating [8, 10, 14].

2.2.2.2. Orientation, cutting and etching. All pulled crystals have been spontaneously nucleated on a platinum rod ($\phi = 2$ mm), and a partially or fully single crystalline state was obtained by necking. The surviving crystals had their (pseudo) tetragonal *c*-axis invariably oriented along the pulling direction. Usually faceting of the tetragonal (1 1 0) planes occurred (Fig. 7).

The crystals were oriented under the microscope by means of the specular reflection of step-like (0 0 1) facets, and (0 0 1) cut platelets were prepared with a thickness of 50 to 100μm.

Figure 7 Fresnoite crystal with 20 at. % Si (nominal) with tetragonal (1 1 0) faceting (scale in cm).

Etching (HCl conc: $C_2H_5OH = 1:1$; 3 min) of the polished platelets (1 μm diamond) invariably showed weak attack of the polishing scratches on the surface oriented towards the pulling direction (Fig. 8a), whereas the scratches became larger, and showed individual, mechanically-induced dislocations on the surface oriented towards the melt (Fig. 8b). This proves the polar saturated character (see Section 1) of the crystals of both the high and low temperature phase and shows that the sign of the axial thermal gradient determines the orientation of the spontaneous dipole at the growth front. For the corresponding sign of the pyroelectric coefficient, see Section 2.2.2.6. No 180° growth domains (twins) were observed.

2.2.2.3. Spontaneous bi-refringence. In order to determine the temperature of the phase transition 4mmFmm2 as a function of the Si/Ge ratio, the spontaneous bi-refringence of the orthorhombic phase perpendicular to the polar axis was measured on a Leitz hot-stage at $\lambda = 546$ nm as a function of temperature (Fig. 9). The bi-refringence

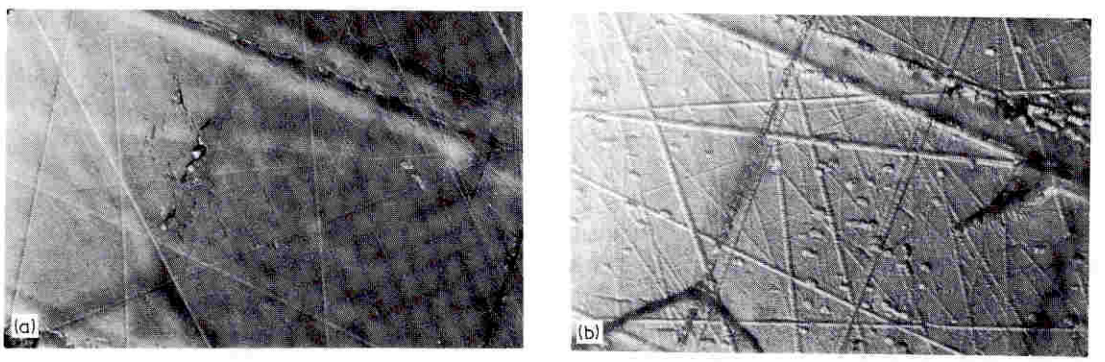

Figure 8 Surface of polished and etched (0 0 1) cut platelet of $Ba_2TiGe_2O_8$. Transmission: (a) weak attack, side of pulling direction, focused on top; (b) strong attack, side towards melt, focused on bottom through upper surface.

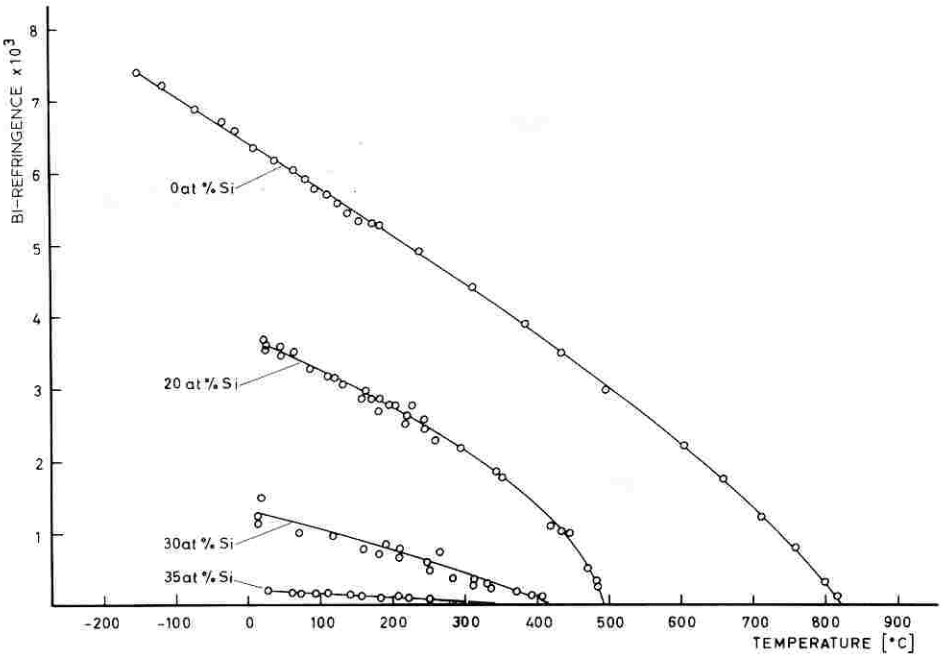

Figure 9 Spontaneous bi-refringence of orthorhombic $Ba_2TiGe_{2-2x}Si_{2x}O_8$ in plane perpendicular to the polar axis versus temperature.

goes smoothly to zero at the transition temperature T_t, showing a second-order type phase transformation. Owing to a decrease of the slope $\partial\Delta n/\partial T$ with increasing Si content, the accuracy of the determination of T_t decreases in this direction. The Δn measurements were made on optically homogeneous regions and the same site of the platelets as used for Δn measurement was also used for the microprobe analysis (see Section 2.2.2.4).

The transition temperature of 830° C found by Δn measurement for $Ba_2TiGe_2O_8$ is consistent with the values 810° C and 850° C corresponding to a minimum of piezoelectric resonance frequency and a bend of the DTA curve [1], respectively.

Whereas the domain patterns of the Ge-fresnoite were characterized by spikes and lamellas (Fig. 4) as reported earlier [1, 15], the orthorhombic domains of the mixed crystals were usually delineated by the walls of the "cells" (Fig. 6).

2.2.2.4. Microprobe analysis. Owing to the smallness of homogeneous single domains within cells of the crystals, X-ray fluorescence analysis was not feasible. Therefore, only X-ray microprobe analysis was possible. Only the germanium contents was determined using the germanium fresnoite as reference, as shown in Table III.

2.2.2.5. Electrical resistance. For quasistatic measurement of the pyroelectric coefficient, the resistivity of the samples versus temperature has to be known. Therefore platelets with continuous gold electrodes have been measured with a "Keithley 417 high speed" picoammeter with a voltage source of 4.8 V and a protective resistance of 510 kΩ in series. The results are plotted in Fig. 10 in terms of resistivity. It can be seen that the activation energy is nearly independent of the Si/Ge ratio. For a dark green tourmaline, which was used for comparison, an activation energy of $E = 0.92$ eV was found.

2.2.2.6. Pyroelectric coefficient. The stability of the orientation of the spontaneous polarization and the high resistivity of the fresnoites (Fig. 10) permitted the use of a quasistatic method, similar to the one described in [16]. Above about 300° C

TABLE III

at. % Ge (nominal)	at. % Ge (microprobe analysis)
100	100 (reference composition)
80	87
70	80
65	62
60	63

The microprobe data may be in error by ± 10%.

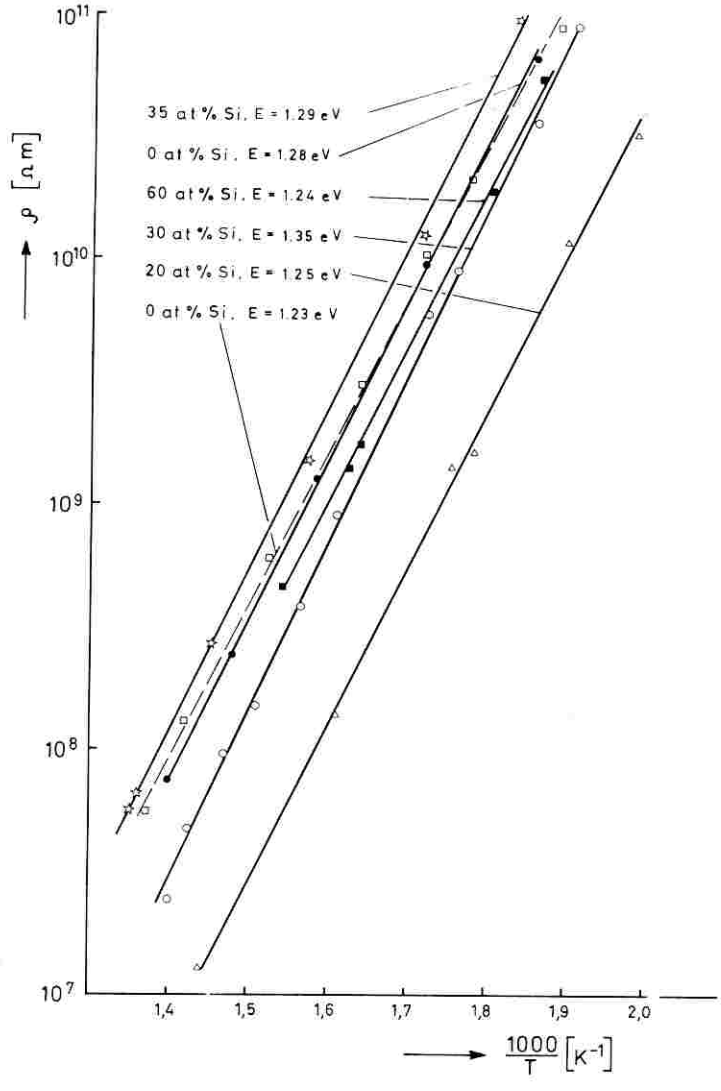

Figure 10 Resistivity (log plot) of several fresnoite compositions versus reciprocal temperature.

a parasitic current became evident, probably owing to a tertiary pyroelectric effect (temperature gradient across thickness). In order to eliminate this component, which depended on T and not on $\partial T/\partial t$, a saw-tooth programme of temperature was used, and the currents I_1 and I_2, corresponding to the heating and cooling slopes, respectively, were measured. Then the pyroelectric coefficient is given by

$$p = (1/A)\frac{I_1 - I_2}{(\partial T_1/\partial t_1) - (\partial T_2/\partial t_2)}$$

where A = surface of sample, I_1 and I_2 are the measuring currents with their sign, and $\partial T_1/\partial t_1$, $\partial T_2/\partial t_2$ the thermal slopes with their sign.

In Fig. 11 the pyroelectric coefficient versus temperature is shown for the compositions with 0, 20, 30, 35 and 60 at.% Si. For testing the equipment, a run with a dark green tourmaline was done, showing a rise from 4 to 6×10^{-6} C m^{-2} K^{-1} between 25 and 350° C, respectively, in good agreement with published data [17, 18] for $T \leqslant$ room temperature. The pyroelectric coefficient of the fresnoites is of the same order of magnitude as that of tourmaline. The same conclusion was recently arrived at also for tetragonal $Ba_2TiSi_2O_8$ [10]. In the Ge/Si fresnoite mixed crystals, the coefficient rises smoothly with temperature and in the sense Ge → Si. The somewhat steeper rise of the compositions with 30 and 35 at.% Si may possibly be caused by the transition to the tetragonal phase.

In pure Ge-fresnoite, the pyroelectric coefficient reverses its sign at about 135° C. This behaviour

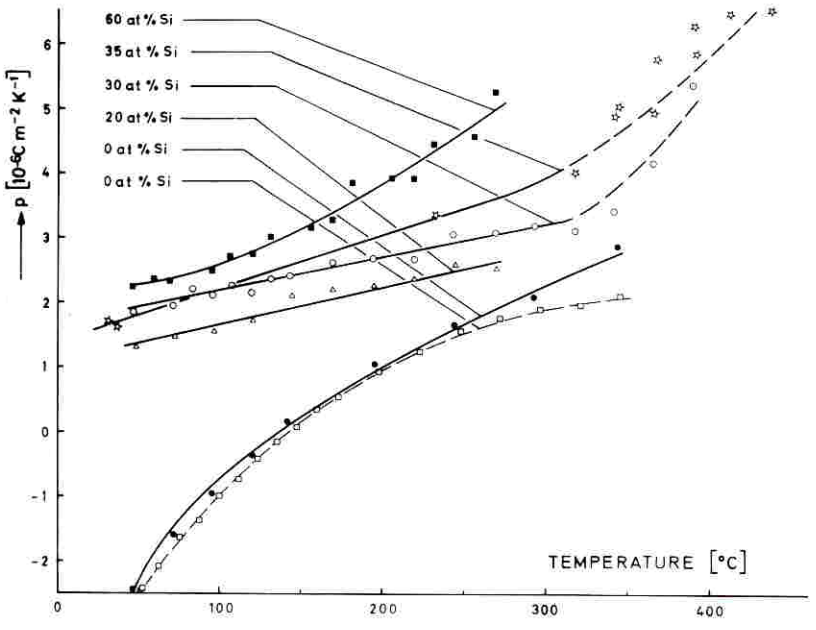

Figure 11 Pyroelectric coefficient of some fresnoite compositions with different Ge/Si ratios.

has been confirmed by means of a second run on another sample. The origin of this phenomenon is not known. Similar, yet unexplained sign reversals of pyroelectric coefficient have become known for several materials, e.g. lithium sulphate, barium nitrate, tourmaline, and cancrinite [18]. Except for the pure Ge-fresnoite, where the reverse is true at room temperature, the pyroelectric charge of all synthesized Ge/Si fresnoites was positive on heating on the crystal face showing weak chemical attack on the polishing scratches.

2.2.2.7. On the symmetry of the orthorhombic phase of $Ba_2TiGe_2O_8$. Buerger precession photographs were taken [19] on orthorhombic single domains, yielding the periods $a_{o.r} \approx b_{o.r} = a_{tetr.} \times \sqrt{2} = 12.27$ Å, and $c_{o.r} = 5.35$ Å, which are consistent with pseudotetragonal [6, 20] and tetragonal [5] powder data, but disagree with the published single crystal data: $a = 12.30$ Å, $b = 135.2$ Å (!), $c = 10.70$ Å [15]. Observation under a polarizing microscope of some "single domains" has revealed mutually slightly misoriented subblocks with extremely small differences in extinction angle, visible only close to the extinction position but not in the too bright 45° position. Examination of such specimens by precession photographs [19] clearly showed large pseudo-identity periods. The literature data [15] are possibly of similar mimicked origin. A more detailed investigation is underway.

Because the phase transformation in Ba_2TiGeO_8 is of second order (see Δn versus T curve, Fig. 7) and the precession photographs of the orthorhombic phase show no change in translations relative to the tetragonal phase [19], the orthorhombic space group should be an equi-translation type sub-group of the tetragonal space group C^2_{4v}–P4bm. There exist only two orthorhombic equi-translation sub-groups of C^2_{4v}–P4bm, namely C^8_{2v}–Pba2 and C^{11}_{2v}–Cmm2 [21, 22]. In the former case, the orthorhombic [1 0 0]/[0 1 0] directions are parallel to the tetragonal [1 0 0]/[0 1 0] directions, whereas in the latter one they run along the tetragonal [1 1 0]/[1 $\bar{1}$ 0] directions. Polarization optical examination has revealed that (i) two of the three indicatrix principal sections run parallel to pseudo-tetragonal (1 1 0) planes (acute bisectrix parallel to the polar axis, optical character positive) and (ii) the orthorhombic domain walls run parallel to the tetragonal (1 0 0) planes. Both facts show that the mirror plane of the tetragonal phase is preserved in the orthorhombic one, leaving us with C^{11}_{2v}–Cmm2 as the only possible space group.

2.2.2.8. Phase diagram. In Fig. 12 a tentative phase diagram for the Ge–Si fresnoite system has been constructed on the basis of various kinds of measuring data. Owing to inhomogeneities of the mixed crystals, the accuracy of the phase boundary between the mm2 and the 4mm phase is

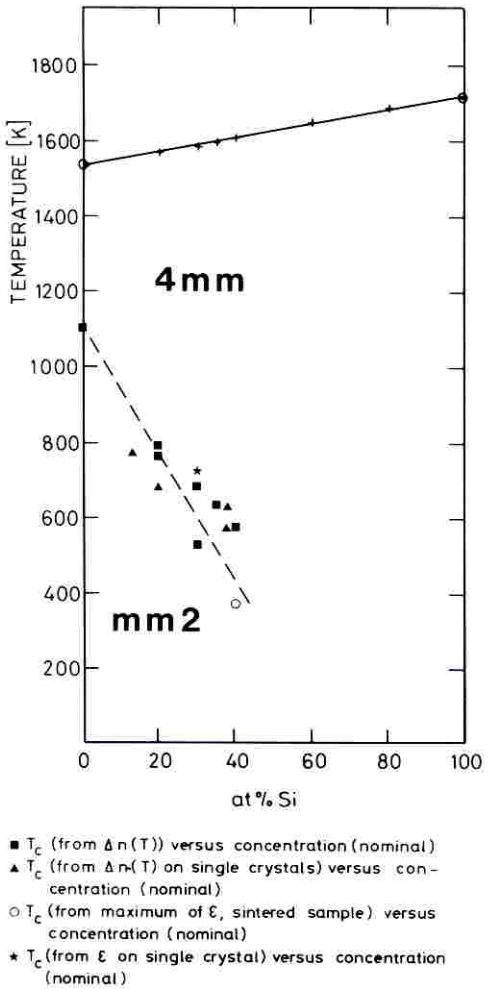

Figure 12 Tentative phase diagram of the fesnoite system $Ba_2TiGe_{2-2x}Si_{2x}O_8$; only melting temperatures as determined from the DTA peaks (4° C min^{-1}) are given. For detail see Fig. 1.

rather poor and will require further refinement; this is likewise true for the solidus curve (Fig. 1).

3. Conclusions

It has been shown that a complete solid solution exists between germanium and silicon fresnoite, and that the phase transition of germanium fresnoite and that of solid solutions between germanium and silicon fresnoite is of the polar/polar type with non-ferroelectric, ferroelastic Aizu species 4mmFmm2. The pyroelectric coefficient in the entire system is of the order of magnitude of that of tourmaline.

Acknowledgement

The authors gratefully acknowledge the support of this work by the D.R.M.E. in Paris and thank Edgar Ascher for illuminating discussions. Thanks are likewise due to Jean-Pierre Rivera, University of Geneva, who kindly made available some X-ray data prior to publication, and to B. O. Hildmann, Technische Hochschule Aachen, for information on $LiNH_4SO_4$.

References

1. M. KIMURA, K. UTSUMI and S. NANAMATSU, *J. Appl. Phys.* **47** (1976) 2249.
2. K. AIZU, *Phys. Rev.* **B2** (1970) 754.
3. B. O. HILDMANN, T. H. HAHN, L. E. CROSS and R. E. NEWNHAM, *Appl. Phys. Lett.* **27** (1975) 103.
4. B. O. HILDMANN, Technische Hochschule Aachen (private communication) (1977).
5. H. E. SWANSON, National Bureau of Standards Monograph No. 25, Section 9 (1971) ASTM card No 22–513.
6. R. MASSE, J.-C. GRENIER and A. DURIF, *Bull. Soc. Minéral. Cristallogr.* **90** (1967) 20.
7. R. MASSE and A. DURIF, *ibid.* **90** (1967) 407.
8. L. E. DRAFALL and K. E. SPEAR, *J. Cryst. Growth* **33** (1976) 180.
9. J. ECKSTEIN, K. RECKER and F. WALLRAFEN, *Naturwiss.* **63** (1976) 435.
10. S. HAUSSÜHL, J. ECKSTEIN, K. RECKER and F. WALLRAFEN, *J. Cryst. Growth* **40** (1977) 200.
11. J. P. M. DAMEN, J. A. PISTORIUS and J. M. ROBERTSON, *Mater. Res. Bull.* **12** (1977) 73.
12. P. HARTMANN, editor, (North Holland, 1973) p. 235.
13. B. R. PAMPLIN, "Crystal Growth" (Pergamon Press, Oxford 1975) p. 43.
14. M. KIMURA, U. FUJINO and T. KAWAMURA, *Appl. Phys. Lett.* **29** (1976) 227.
15. M. KIMURA, K. DOI, S. NANAMATSU and T. KAWAMURA, *ibid.* **23** (1973) 531.
16. R. L. BYER and C. B. ROUNDY, *Ferroelectrics* **3** (1972) 333.
17. S. B. LANG, "Sourcebook of Pyroelectricity" (Gordon and Breach, New York, 1974).
18. S. N. DROZHDIN, V. K. NOVIK, V. A. KOPSIK and I. B. KOBIAKOV, *Fiz. Tverd. Tela* **16** (1974) 3266.
19. J.-P. RIVERA, University of Geneva (private communication) (1977).
20. J. P. GUHA, *J. Amer. Ceram. Soc.* **60** (1977) 246.
21. E. ASCHER, "Lattices of equi-translation subgroups of the space groups" (Battelle Institute, Advanced Studies Centre, Geneva, Switzerland, 1968).
22. J. NEUBÜSER and H. WONDRASCHEK, "Maximal subgroups of the space groups" (corrected 1977) (Kiel and Karlsruhe Universities, 1969).

Received 30 December 1977 and accepted 15 February 1978.